NANO LETTERS

Letter

pubs.acs.org/NanoLett

Self-Powered, Ultrasensitive, Flexible Tactile Sensors Based on Contact Electrification

Guang Zhu,[†,§,∥] Wei Qing Yang,[†,‡,∥] Tiejun Zhang,[†] Qingshen Jing,[†] Jun Chen,[†] Yu Sheng Zhou,[†] Peng Bai,[†] and Zhong Lin Wang*[,†,§]

[†]School of Materials Science and Engineering, Georgia Institute of Technology, Atlanta, Georgia 30332, United States

[‡]State Key Laboratory of Electronic Thin Films and Integrated Devices, University of Electronic Science and Technology of China, Chengdu 610054, China

[§]Beijing Institute of Nanoenergy and Nanosystems, Chinese Academy of Sciences, Beijing 100083, China

S *Supporting Information*

ABSTRACT: Tactile/touch sensing is essential in developing human-machine interfacing and electronic skins for areas such as automation, security, and medical care. Here, we report a self-powered triboelectric sensor based on flexible thin-film materials. It relies on contact electrification to generate a voltage signal in response to a physical contact without using an external power supply. Enabled by the unique sensing mechanism and surface modification by polymer-nanowires, the triboelectric sensor shows an exceptional pressure sensitivity of 44 mV/Pa (0.09% Pa^{-1}) and a maximum touch sensitivity of 1.1 V/Pa (2.3% Pa^{-1}) in the extremely low-pressure region (<0.15 KPa). Through integration of the sensor with a signal-processing circuit, a complete tactile sensing system is further developed. Diverse applications of the system are demonstrated, explicitly indicating a variety of immediate uses in human-electronics interface, automatic control, surveillance, remote operation, and security systems.

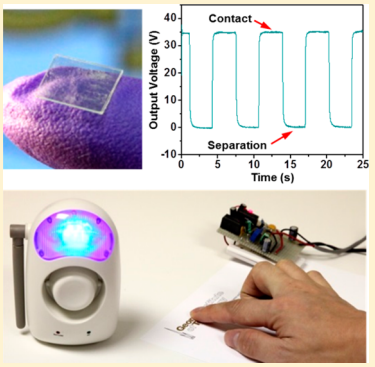

KEYWORDS: *Contact electrification, self-powered electronics, tactile sensing, flexible electronics*

Tactile (or touch) sensing is a field that is rapidly advancing as driven by vast applications including human-machine interfacing, skin-like electronics, industrial automation, medical procedures, and security systems.[1−8] Tactile sensors, according to transducing mechanisms, can be divided into the following major categories: capacitive,[9,10] piezoelectric,[11−13] resistive,[14−16] and optical.[17] All of these mechanisms rely on deformation of the sensing unit in response to interaction with an object. Such a deformation-dependence poses a challenge in touch detection when very weak interaction is involved. Another major limitation of aforementioned sensors is that they all require an external power supply to generate an electrical parameter for characterizing the output of the sensor; otherwise none of them can normally operate. This causes problems such as power consumption and structural complexity.[18] Besides, fragility, stiffness, and high cost are also common concerns that impair widespread adoption of tactile sensors.[18−20] Here we report a new class of self-powered triboelectric sensor (TES). The thin-film-based TES utilizes contact electrification to generate a voltage signal in response to a physical contact without reliance on an external power supply, completely resolving the issue of power consumption for the sensing unit. Enabled by the novel sensing mechanism and surface modification/functionalization based on polymer-nanowires, the TES showed an exceptional pressure sensitivity of 44 mV/Pa (0.09% Pa^{-1}) and a maximum touch sensitivity of 1.1 V/Pa (2.3% Pa^{-1}) in extremely low-pressure region (<0.15 KPa). Since contact electrification is universally applicable to any material, the TES can effectively respond to either insulating or conductive materials of all kinds. Having a flexible structure, it can be tailored to any size, shape, and color/colorless, making it adaptive to even curved surfaces. More importantly, through integration of the TES with a signal-processing circuit, a complete tactile sensing system was developed. Diverse applications of the system were demonstrated, explicitly indicating a variety of immediate uses in human-electronics interface, automatic control, surveillance, remote operation, and security systems. Considering that the TES features other major advantages in scalability, durability, cost, and implementation, it therefore opens up a new paradigm for widespread adoption of tactile sensing.

A TES is composed of thin-film materials that are vertically laminated (Figure 1a). A layer of polyethylene terephthalate (PET) forms the structural backbone of the TES, which is sandwiched by transparent ITO layers as electrodes on both sides. On the top side, a layer of fluorinated ethylene propylene (FEP) is applied as an electrification layer that generates triboelectric charges upon contact with a foreign object. Surface modification on the FEP could be adopted to create vertically aligned polymer nanowires (PNWs) (Figure 1b). They have an

Received: February 12, 2014
Revised: April 14, 2014

   dx.doi.org/10.1021/nl5005652 | *Nano Lett.* XXXX, XXX, XXX−XXX

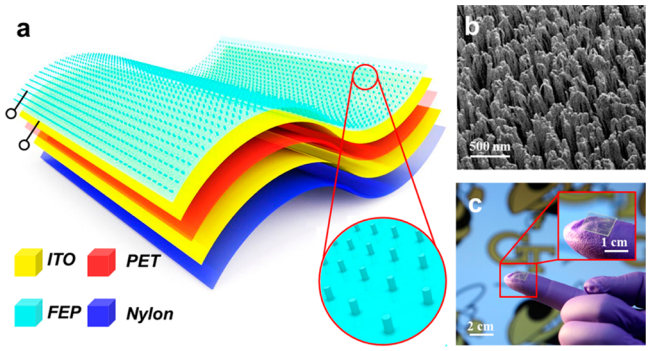

Figure 1. Structural design of the TES. (a) Schematic illustration of the TES. Inset: enlarged schematic of polymer nanowires on the top surface. (b) SEM image of polymer nanowires created by plasma dry etching. (c) Photograph of an as-fabricated TES.

average diameter and length of 150 nm and 1.5 μm, respectively, which play an important role in achieving high sensitivity for low pressure detection, as will be discussed in later sections. On the bottom side, a nylon film serves as a protection layer due to its outstanding mechanical and thermal properties. A photograph of an as-fabricated TES is shown in Figure 1c. Made of conventional thin-film materials, the TES has an extremely low cost, which is advantageous for its practicability. The structural design, as well as the fabrication process, is compatible to possible large-scale manufacturing.

The self-powered operating principle of the TES can be explained by the coupling effect between contact electrification and electrostatic induction. Because of the large composition percentage of fluorine that has the highest electronegativity among all elements, the FEP is one of the most triboelectric-negative materials.[21] It always tends to gain negative charges when in contact with almost any other materials. At the "contact state" in which a foreign object is in touch with the TES (Figure 2a), triboelectric charges are generated at the contact surfaces, with negative ones on the TES side and positive ones on the object side.[22] They are balanced by their opposite counterparts, which does not induce an open-circuit voltage across the two electrodes. At the "separation state" when the object is absent (Figure 2b), the negative triboelectric charges do not annihilate but remain on the surface of the TES for an extended period of time.[23] These charges introduce a net electric field between the two electrodes. Since the top electrode is closer to the negative charges than the bottom electrode (Figure 2c), it possesses a lower electric potential compared to the bottom one. Considering that the top and the bottom electrodes are connected to the positive and the negative terminals of a measurement system, the open-circuit voltage across the electrodes at the separation state can be analytically expressed by eq 1 below.

$$V = U_{\text{top}} - U_{\text{bottom}} = \frac{-\sigma t}{2\varepsilon_0 \varepsilon_r} \tag{1}$$

where U_{top} is the electric potential of the top electrode, U_{bottom} is the electric potential of the bottom electrode, $-\sigma$ is the negative triboelectric charge density on the FEP, t is the distance between the two electrodes that is equivalent to the PET substrate thickness, ε_0 is the dielectric constant of vacuum, and ε_r is the relative permittivity of PET. On the basis of this equation, the separation and the contact states correspond to the minimum and the maximum values of the open-circuit voltage, respectively. The independence of an external power supply for electric signal generation is an unparalleled feature compared to any other tactile sensing technique.

To characterize the response of the TES to a contact event, we used the output voltage defined as the difference of the open-circuit voltage with respect to that at the separation state. Consequently, the output voltage always has a positive value, which has a zero-baseline corresponding to the separation state. Here, a square-shaped TES having an edge length of 5 cm was utilized to detect a metal object with a planar dimension of 2.5 cm by 2.5 cm. Repetitive contact and separation were realized through a linear motor that provided a precisely controlled reciprocating motion. Details on measurement setup as well as sample preparation are presented in Methods. As shown in Figure 3a, at a contact force of 20 mN (applied pressure of 0.03 KPa) the TES produces a uniform square-wave output voltage with the maximum amplitude of 35 V.

As the contact force/pressure increases, the output voltage rises and finally saturates at 50 V when the contact pressure approaches 10 KPa (Figure 3b). This increasing behavior can be attributed to the increase of contact area. High pressure results in more contact area, which imparts higher density of surface charges to the TES.[24] As a result, higher output voltage is obtained. It is noticed that the curve in Figure 3b exhibits two distinct regions. In the extremely low-pressure region (<0.15 KPa), an exceptional pressure sensitivity[25] of 44 mV/Pa is achieved with excellent linearity (R^2 = 0.991), corresponding to a sensitivity factor of 0.09% Pa^{-1}. In the region beyond 2 KPa, the pressure sensitivity drops to 0.5 mV/Pa but still has good linearity (R^2 = 0.974). It is suggested that the two-region behavior is likely due to the enhancement effect resulting from the PNWs on the TES surface. The sensed object has surface

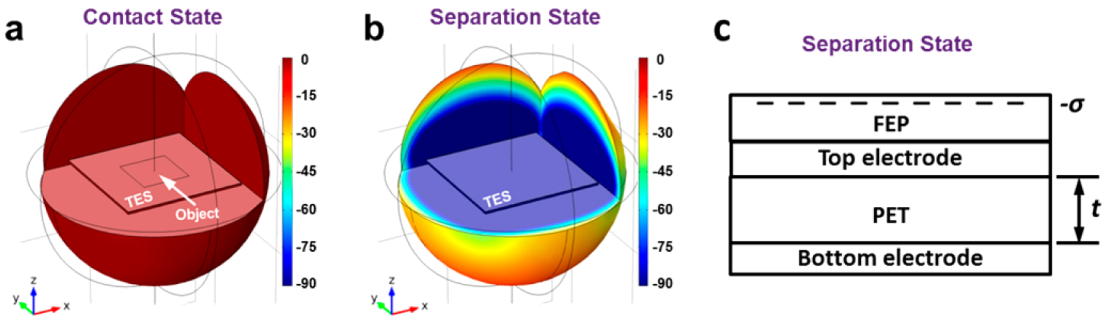

Figure 2. Operating principle of the TES. (a) Three-dimensional potential distribution at the contact state with a contact object in touch with the TES. (b) Three-dimensional potential distribution at the separation state without the object. (c) Two-dimensional cross-sectional view of the TES at the separation sate.

dx.doi.org/10.1021/nl5005652 | Nano Lett. XXXX, XXX, XXX−XXX

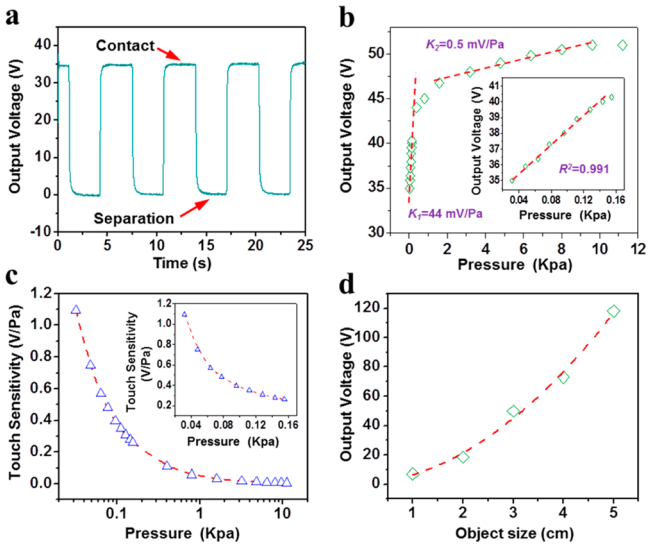

Figure 3. Characterization results of the TES. (a) Output voltage at a contact pressure of 0.03 KPa from a TES (5 cm in side length) when sensing a metal object (2.5 cm in side length). (b) Output voltage with increasing pressure. Inset: enlarged view in small-pressure region. (c) Touch sensitivity with increasing pressure. Inset: enlarged view in small-pressure region. (d) Output voltage with increasing the size of the metal object at a uniform pressure of 0.03 KPa. The TES has a fixed side length of 5 cm.

asperities at micro- and nanoscale, as revealed in Figure S1, Supporting Information. Without the PNWs, the contact between two nominal flat surfaces is confined at certain points due to the surface asperities. In comparison, the high-aspect-ratio PNWs are likely to be readily bent and become adaptive to the morphology of the sensed object in a weak contact. Such a conformable interaction can result in a largely enhanced increment of the real contact area in response to an increase of the pressure because it requires much less pressure to deform the PNWs than the bulk FEP film. As a result, the device with the PNWs exhibits a much more sensitive response in the low-pressure region (<0.15 KPa). As shown in Figure S2, Supporting Information, the nanowire-based modification leads to a 7-fold enhancement in the pressure sensitivity for ultralow pressure detection. It needs to be noted that a proper length of the PNWs is important for the sensitivity enhancement. On one hand, the enhancement was not observed for short PNWs (~600 nm in Figure S3a, Supporting Information) due to possibly ineffective interaction with the contact object. On the other hand, excessively long PNWs (>3 μm) tend to fall down after a number of contacts (Figure S3b, Supporting Information), which reveals poor mechanical robustness.

To further characterize the ability of the TES in responding to a contact event, touch sensitivity[26] is calculated and plotted in Figure 3c. The touch sensitivity reaches an ultrahigh value of 1.1 V/Pa, corresponding to a factor of 2.3% Pa^{-1}. It indicates the superior applicability of the TES in detecting a touch event especially when the interaction is week. It is found that the PNW-based modification can also largely promote the touch sensitivity by as much as 150% compared to the device without the modification (Figure S4, Supporting Information). As discussed above, the PNWs can possibly increase the number of contact points by accommodating the surface asperities by the comfortable interaction. Compared to recent reports on plastic thin-film pressure sensors,[10,12,15,16,27−31] our device demonstrates unprecedented sensitivity in an extremely low-pressure region (<0.15 KPa) where interaction is at least 2 orders of magnitude weaker than a gentle finger touch.[5]

The size is a major factor that determines the output voltage as well as the sensitivity of the TES. For a TES with a fixed size (5 cm in side length), a quadratic increase in output voltage is obtained with respect to side length of the sensed object that varies from 1 to 5 cm (Figure 3d). Alternatively, the output voltage linearly scales with the object area. The reason is that a larger object imparts more triboelectric charges to the TES, which induces a higher potential in magnitude on the upper electrode given that the electrode has a fixed area. The proposed explanation is further supported by results in Figure S4a, Supporting Information, in which the output voltage is reversely proportional to the device area, while the sensed object has a fixed size. If both the TES and the object scale altogether, the output voltage keeps stable (Figure S5, Supporting Information). Therefore, an important guidance in achieving high sensitivity is that the TES needs to have a lateral dimension smaller than an object that is to be detected.

The TES can still be fully functional when the lateral dimension is scaled down to microscale. Equation 1 is based on the assumptions that the FEP surface is infinitely large and uniformly charged. These assumptions can hold true only on the condition that the lateral dimension is far larger than the PET thickness. If the TES is substantially scaled down, the edge effect can become dominant. Then the electric field between the two electrodes is not uniform anymore. As a result, the magnitude of the open-circuit voltage will drop, as shown in Figure 4a based on the COMSOL simulation data. At macro-

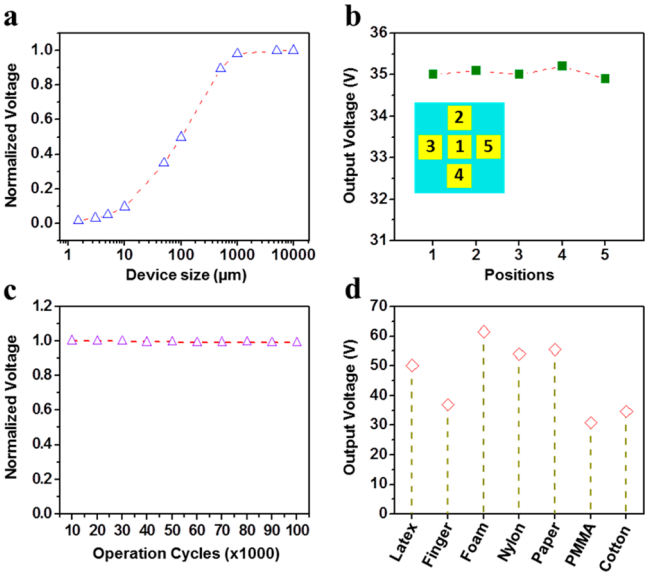

Figure 4. Electric measurement results that demonstrate the advantages of the TES. (a) Normalized output voltage as a functional of the lateral dimension of the TES. The results are obtained by COMOSL simulation. (b) Distribution of output voltage when a metal object (1 cm in side length) contacts at different positions on the TES (5 cm in side length) at a contact pressure of 0.03 KPa. Inset: a top-view schematic that illustrates the five contact locations on the TES. (c) Results of durability test on the TES (5 cm in side length) for sensing a metal object (2.5 cm in length) at a contact pressure of 20 KPa. (d) Output voltage of the TES (5 cm in side length) in response to different contact materials (2.5 cm in side length) at a uniform contact pressure of 0.03 KPa.

dx.doi.org/10.1021/nl5005652 | Nano Lett. XXXX, XXX, XXX−XXX

scale, the output voltage is independent of the lateral dimension, which is consistent with eq 1. However, as the lateral dimension is scaled down to below 10 times the PET thickness (<500 μm), the output voltage starts to substantially drop. The normalized voltage decreases to 0.5 and 0.1 when the lateral dimension shrinks to 100 and 10 μm, respectively. The output voltage can still reach about 3.5 V for a pixel size as small as 10 μm, which can be easily measured.

In addition to ultrahigh sensitivity and self-generated output, the TES features a number of other merits. An important aspect in evaluating a tactile sensor is the output dependence on locations where a touch event takes place. Figure 4b presents values of output voltage at 5 different locations where the TES (5 cm in side length) interacts with a metal object having a side length of 1 cm. The five locations are depicted in the inset of Figure 4b. The output proves to be independent of the location, which is indicative of uniform sensing when addressing small-sized objects. Moreover, the TES has a robust structure and is made from durable materials. As a result, it owns excellent durability. After repetitive contacts for 10^5 cycles at a frequency of 1 Hz with a pressure of 20 KPa, the output voltage shows only a slight fluctuation within 1% (Figure 4c). The output voltage is independent of the contact frequency considering that the surface triboelectric charges dissipate very slowly and that they can be replenished in each contact even though the dissipation is significant. Additionally, the TES is generally applicable to objects that are made of various materials. Figure 4d presents a survey of outputs in response to materials that are commonly found for daily usage, which reveals the widespread applicability of the TES in a variety of circumstances.

The large voltage signal induced by a contact event can be easily picked up by external readout circuits. For practical applications, a complete wireless sensing system was developed through integrating the TES with a signal-processing circuit. As diagramed in Figure S6, Supporting Information, the system relies on the output voltage from the TES to trigger an IC timer that controls a wireless transmitter for remotely switching a siren between a panic state and a silence state. In the first demonstration shown in Figure 5a, a TES was customized to a dimension of 1 cm by 1 cm. Once a human finger gently contacted the TES, the output voltage (Figure 5b) touched off the siren that produced a sharp alarm with flashing light (Figure 5b and Supplementary Movie 1, Supporting Information). In the second demonstration, a square-shaped TES with side length of 10 cm was laid on the ground and imbedded underneath a piece of carpet (Figure 5c). When a person stepped on top of the TES as walking by, an output voltage of 15 V shown in Figure 5d was generated even though the shoe did not have an intimate contact with the TES. This was because the TES was loosely covered by the carpet, leaving a spatial gap between them. When the carpet was pressed down by the human foot, it fully touched the TES. Such a variance in contact area would give an output voltage from the TES, which then triggered the siren (Figure 5c and Supplementary Movie 2, Supporting Information). Moreover, the sensing system could be applied to other circumstances, such as a door handle (Figure 5e). For this particular scenario, the TES was tailored to a long strip (5 cm by 3 mm) and fixed on the curved surface of the handle, exhibiting its ability in adapting to different shapes for flexible implementation. As demonstrated in Figure 5e and Supplementary Movie 3, Supporting Information, the sensing system immediately started operation once a human

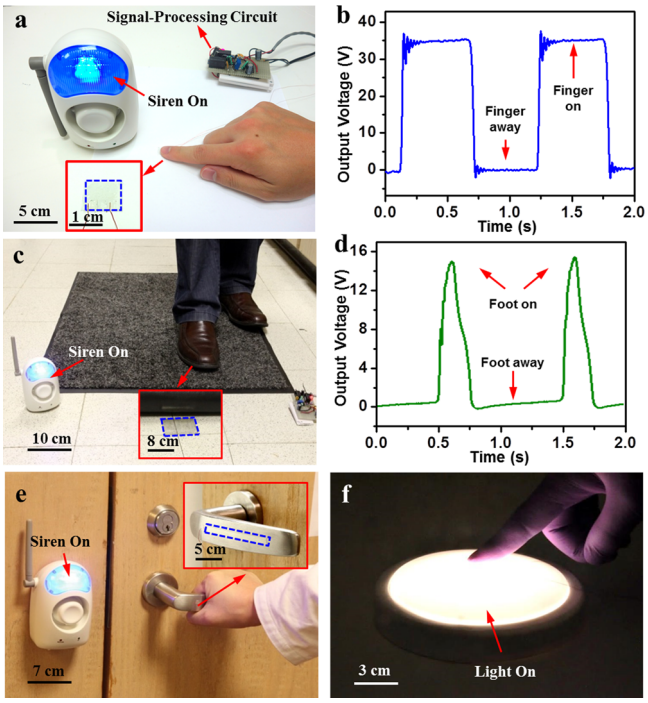

Figure 5. Complete sensing system based on the TES for practical applications. (a) Triggering a wireless alarm system by gentle finger tapping on a TES (1 cm in side length). Inset: enlarged view of the TES on a piece of paper. (b) Output voltage of the TES generated by finger tapping. (c) Triggering a wireless alarm system by stepping on top of a TES (10 cm in side length) that is embedded underneath a carpet. Inset: enlarged view of the TES on the floor. (d) Output voltage generated by stepping on the TES covered by the carpet. (e) Triggering a wireless alarm system by grabbing the TES (5 cm by 3 mm) that is applied on a door handle. Inset: enlarged view of the TES on the door handle. (f) Switching a panel light by finger tapping on the TES (1 cm in side length) that is applied on the surface of the light.

hand grabbed the door handle. Through a minor revision that substitutes other functional electronics for the wireless transmitter in the electric diagram (Figure S7, Supporting Information), the sensing system could be adopted for more purposes. For example, it was demonstrated as a touch-enabled switch for a panel light, which is shown in Figure 5f and Supplementary Movie 4, Supporting Information. Therefore, the TES along with the sensing system developed here has immediate applications in a variety of areas, including human–machine interface, automatic control, surveillance, remote operation, and security systems.

In summary, we developed a novel thin-film-based triboelectric sensor (TES) for ultrasensitive tactile sensing without an external power source. From a fundamental innovation point of view, the TES relies on triboelectrification resulting from a contact event to generate an output voltage and does not consume any electric energy from an external power source. Thus, the self-powered TES represents a breakthrough concept for tactile sensing/imaging. From a device performance point of view, because of the novel sensing mechanism as well as diverse surface chemical and physical modifications on PNWs, the TES has achieved an ultrahigh level of pressure sensitivity as well as touch sensitivity in an extremely low-pressure region. Besides, high levels of uniformity, stability, and applicability have also been achieved. Finally, from a practical application point of view, a complete sensing system was built through integrating a

dx.doi.org/10.1021/nl5005652 | Nano Lett. XXXX, XXX, XXX–XXX

TES with a signal-processing circuit. A variety of applications were demonstrated, in which the TES could sensitively trigger functional electronics in response to common external excitations, such as finger touching, hand grabbing, and foot pressing. Considering that the TES features other major advantages in scalability, cost, and implementation, it has a promising prospect for robotics, human−machine interfacing, and security.

Methods. *Fabrication of a TES.* 1. Prepare a PET substrate of 50 μm thickness with a desired dimension using laser cutting. 2. Deposit 150 nm of ITO on both sides of the PET as electrodes using a RF sputterer. 3. Connect a lead wire to each of the electrodes. 4. Adhere a nylon thin film (50 μm) on one side of the device as a protection layer. 5. Adhere a FEP thin film (50 μm) on the other side of the device as an electrification layer. 6. Create vertically aligned polymer nanowires on the FEP surface using plasma dry etching.[32]

Fabrication of Contact Objects. 1. Prepare an acrylic sheet of 1.5 mm in thickness as a substrate with a desired dimension using laser cutting. 2. For the contact object made of metal, adhere a layer of Kapton film (125 μm) on the substrate and then deposit 200 nm of copper on top of the polymer surface using a DC sputterer. 3. For other contact objects, adhere a layer of target materials that are commercially available on one side of the substrate.

Measurement Setup. 1. Mount the TES vertically on a three-dimensional positioner that also has control on rotation and tilt. 2. Align and connect the contact object with a force sensor. 3. Vertically mount the force sensor along with the contact object to one end of a linear motor for reciprocating motion. 4. Adjust the three-dimensional positioner so that the TES surface and the object surface are parallel to each other. 5. Simultaneously monitor the TES output using an electrometer and the interaction force between TES and the object. 6. Change the interaction force through incrementally changing stroke distance of the linear motor to investigate the dependence of voltage on contact pressure.

■ ASSOCIATED CONTENT

Supporting Information

Supplementary figures and movies. This material is available free of charge via the Internet at http://pubs.acs.org.

■ AUTHOR INFORMATION

Corresponding Author

*(Z.L.W.) E-mail: zhong.wang@mse.gatech.edu.

Author Contributions

∥(G.Z. and W.Q.Y.) These authors contributed equally to this work.

Notes

The authors declare no competing financial interest.

■ ACKNOWLEDGMENTS

Research was supported by U.S. Department of Energy, Office of Basic Energy Sciences (Award DE-FG02-07ER46394), and the "thousands talents" program for pioneer researcher and his innovation team, China, Beijing City Committee of Science and Technology projects (Z131100006013004 and Z131100006013005). Patents have been filed based on the research results presented in this manuscript.

■ REFERENCES

(1) Kim, D.-H.; et al. Epidermal electronics. *Science* **2011**, *333*, 838−843.

(2) Dargahi, F.; Najarian, S. Advanced in tactile sensors design/manufacturing and its impact on robotics applications. *Ind. Rob.* **2005**, *32*, 268−281.

(3) Tiwana, M. I.; Redmond, S. J.; Lovell, N. H. A review of tactile sensing technologies with applications in biomedical engineering. *Sens. Actuators, A* **2012**, *179*, 17−31.

(4) Kaltenbrunner, M.; et al. An ultra-lightweight design for imperceptible plastic electronics. *Nature* **2013**, *499*, 458−465.

(5) Mannsfeld, S. C. B.; et al. Highly sensitive flexible pressure sensors with microstructured rubber dielectric layers. *Nat. Mater.* **2010**, *9*, 859−865.

(6) Schwartz, G.; et al. Flexible polymer transistors with high pressure sensitivity for application in electronic skin and health monitoring. *Nat. Commun.* **2013**, *4*, No. 1859.

(7) Maheshwari, V.; Saraf, R. F. High-resolution thin-film device to sense texture by touch. *Science* **2006**, *312*, 1501−1504.

(8) Manunza, I.; Sulis, A.; Bonfiglio, A. Pressure sensing by flexible, organic, field effect transistors. *Appl. Phys. Lett.* **2006**, *89*, 143502.

(9) Lee, H.-K.; Change, S.-I.; Yoon, E. A flexible polymer tactile sensor: fabrication and modular expandability for large area deployment. *J. Microelectromech. Syst.* **2006**, *25*, 1681−1686.

(10) Metzger, C.; et al. Flexible-foam-based capacitive sensor arrays for object detection at low cost. *Appl. Phys. Lett.* **2008**, *92*, 013506.

(11) Dahiya, R. S.; Metta, G.; Valle, M.; Adami, A.; Lorenzelli, L. Piezoelectric oxide semiconductor field effect transistor touch sensing devices. *Appl. Phys. Lett.* **2009**, *95*, 034105.

(12) Shirinov, A. V.; Schomburg, W. K. Pressure sensor from a PVDF film. *Sens. Actuators, A* **2008**, *142*, 48−55.

(13) Park, K. I. Highly efficient, flexible piezoelectric PZT thin film nanogenerator on plastic substrate. *Adv. Mater.* **2014**, *26*, 2514−2520.

(14) Zhang, H.; So, E. Hybrid resistive tactile sensing. *IEEE Trans. Syst. Man Cybern., Part B* **2002**, *32*, 57−65.

(15) Hussain, M.; Choa, Y.-H.; Nihara, K. Conductive rubber materials for pressure sensors. *J. Mater. Sci. Lett.* **2001**, *20*, 525−527.

(16) Shimojo, M.; Namiki, A.; Ishikawa, M.; Makino, R.; Mabuchi, K. A tactile sensor sheet using pressure conductive rubber with electrical-wires stitched method. *IEEE Sens. J.* **2004**, *4*, 589−596.

(17) Heo, J.-S.; Chung, J.-H.; Lee, J.-J. Tactile sensor arrays using fiber Bragg grating sensors. *Sens. Actuators, A.* **2006**, *126*, 312−327.

(18) Rocha, J. G.; Lanceros-Mendez, S. *Sensors: Focus on Tactile Force and Stress Sensors*; I-Tech Publishers: Vienna, Germany, 2008.

(19) Siciliano, B.; Khatib, O. *Handbook of Robotics*; Springer: Berlin, Germany, 2008.

(20) Dahiya, R. S.; Valle, M. *Robotic Tactile Sensing*; Springer: Berlin, Germany, 2013.

(21) Wang, Z. L. Triboelectric nanogenerators as new energy technology for self-powered systems and as active mechanical and chemical sensors. *ACS Nano* **2013**, *7*, 9533−9557.

(22) Zhu, G.; et al. Triboelectric-generator-driven pulse electrodeposition for micro-patterning. *Nano Lett.* **2012**, *12*, 4960−4965.

(23) Zhou, Y. S.; et al. In-situ quantitative study of nanoscale triboelectrification and patterning. *Nano Lett.* **2013**, *13*, 2771−2776.

(24) Zhu, G.; et al. Toward large-scale energy harvesting by a nanoparticle-enhanced triboelectric nanogenerator. *Nano Lett.* **2013**, *13*, 847−853.

(25) The pressure sensitivity is used to characterize the response to pressure change and is defined as $S_p = \delta V/\delta p$ (mV/Pa), where V denotes the output voltage, and p denotes the applied pressure. The pressure sensitivity factor is defined as $S_{p\text{-factor}} = \delta[(V_m - V)/V_0]/\delta p$ (Pa^{-1}), where V_m denotes the maximum output voltage.

(26) The touch sensitivity is used to characterize the response to a touch event and is defined as $S_t = \Delta V/\Delta p = (V - V_0)/(p - p_0)$ (mV/Pa), where V_0 denotes the output voltage without contact ($V_0 = 0$), and p_0 denotes the applied pressure without contact ($p_0 = 0$). Thus, $S_t = V/p$. The touch sensitivity factor is expressed as $S_{t\text{-factor}} = [(V_m - V)/V_m]/p$ (Pa^{-1}).

(27) Wen, Z.; et al. Development of an integrated vacuum microelectronic tactile sensor array. *Sens. Actuators, A* **2003**, *03*, 301−306.
(28) Nadvi, G. S.; Butler, D. P.; Celik-Butler, Z.; Gonenli, I. E. Micromachined force sensors using thin film nickel-chromium piezoresistors. *J. Micromech. Microeng.* **2012**, *22*, 065002.
(29) Pang, C.; et al. A flexible and highly sensitive strain-gauge sensor using reversible interlocking of nanofibres. *Nat. Mater.* **2012**, *11*, 795−801.
(30) Darlinski, G.; Bottger, U.; Waser, R. Mechanical force sensors using organic thin-film transistors. *J. Appl. Phys.* **2005**, *97*, 093708.
(31) Someya, T.; et al. A large-area, flexible pressure sensor matrix with organic field-effect transistors for artificial skin applications. *Proc. Natl. Acad. Sci.* **2004**, *101*, 9966−9970.
(32) Fang, H.; Wu, W.; Song, J.; Wang, Z. L. Controlled growth of aligned polymer nanowires. *J. Phys. Chem. C* **2009**, *113*, 16571−16574.

dx.doi.org/10.1021/nl5005652 | *Nano Lett.* XXXX, XXX, XXX−XXX